Comparative Analysis of Bamboo-based (*Bambusa vulgaris*) Activated Carbon produced through Trioxonitrate (V) Acid and Potassium Hydroxide

C.O. Akinbile*, E. M. Epebinu, O.O. Olanrewaju, A.T. Abolude

Department of Agricultural & Environmental Engineering, Federal University of Technology, Akure, Nigeria.

ABSTRACT: Activated carbon (AC) is one of the numerous cost-effective inputs for treating wastewater in an efficient and cost-effective manner, and several materials have been used to produce AC with diverse results. One such material with a large potential is African Bamboo (*Bambusa vulgaris*), especially due to its availability. In this study, bamboo was carbonized and then activated using trioxonitrate (V) acid (HNO_3) and potassium hydroxide (KOH) as activating agents. The AC was characterized using Fourier Transform Infrared Spectroscopy (FTIR) and Scanning Electron Microscopy (SEM) technologies at 50 µm, 80 µm, 100 µm, and 200 µm magnification. The SEM imagery results at 50 µm and 1500x magnification showed that the AC produced using KOH had the largest and most well-developed pore spaces hence maximum capacity to absorb contaminants compared to HNO_3's AC and inactivated carbonated charcoal. The FTIR spectra peak analysis results also confirmed that KOH's AC had the highest number of functional groups on its surface and, therefore, enhanced its adsorption capacity.

KEYWORDS: Bamboo; Activated Carbon; FTIR; SEM; Adsorption capacity.

[Received Nov. 24, 2022; Revised April 04, 2023; Accepted April 04, 2023] Print ISSN: 0189-9546 | Online ISSN: 2437-2110

I. INTRODUCTION

Bamboo is a potentially renewable biomass resource which can be converted into bio-fuels and bio-chemicals by thermochemical conversion technology (Ma *et al*, 2019) it belongs to the family (*Gramineae*, subfamily *Bambusoideae*) and has over 1200 species worldwide sitting on approximately 22 million ha bamboo forest areas globally (Zhou, 1998). The two commonest species of Bamboo in Nigeria are *Bambusa vulgaris* and *Oxystenanthera abyssynica*. *Bambusa vulgaris* attains an average height of between 14-20 meters in 4 to 8 years at maturity. *Oxystenanthera abyssynica* reaches between 8-12 meters at maturity (Omiyale, 2013). *Bambusa vulgaris* grows in a wild forest region and nearby streams in Nigeria and is abundant in the Niger Delta region (Awoyale *et al* 2013). Bamboo's specific gravity and mechanical strength are considered as its assets, making it a sort of renewable organic resource for sustainable development. Bamboo can undergo chemical processing methods which include distilling from bamboo leaves and the pyrolysis of bamboo to get bamboo charcoal and bamboo vinegar (Jiang, 2004). The best time to subject it to pyrolysis is during the 5th year or more of its maturity period (Ijaola *et al*, 2013). Charcoal from Bamboo, therefore, is a micro-porous material with excellent adsorption properties for its large specific surface area (Jiang, 2004) with a high total pore volume distributed in the micropore range. The extra-ordinary microstructure of the Bamboo helps to purify water (Ijaola *et al*, 2013) which makes Bamboo charcoal a potentially cheaper alternative adsorbent among many carbon-based materials such as carbon nanotubes, graphene and graphene oxide.

Globally, over 85% of wastewater released into the environment is untreated and, the bulk of which is from Africa, and contributing considerably to the degradation of water quality (WWAP, 2017). The ineffective treatment, especially in developing countries, may be attributed to a lack of financial resources for the development of sophisticated treatment facilities and techniques. Many important wastewater treatment techniques such as reverse osmosis, ion exchange, electrodialysis, electrolysis, etc are found to be limited due to their expensive operational cost, the high energy requirement for the process, and toxic sludge generation which could present treatment and disposal problem (Awoyale *et al*, 2013). Low-cost techniques such as constructed wetland and adsorption processes require low or no energy for their operation. However, constructed wetlands are land-intensive and clogging of the system may easily occur. With treatments through adsorption, the process involves simple treatment design, no sludge generation, and low capital intensity when compared to other methods of wastewater treatment (Awoyale *et al*, 2013). The adsorption process is the accumulation of liquid or gas contaminants on the surface of a solid substrate. The process is an environmentally friendly and effective treatment option. Several biochar and activated carbons are prepared from the cellulose fraction of some agricultural wastes (linen, cotton and wheat) (Chouikhi *et al*, 2021). Activated carbon (AC) is widely used as an adsorbent for this

*Corresponding author: coakinbile@futa.edu.ng

doi: http://dx.doi.org/10.4314/njtd.v18i4.1155

process due to its high adsorption capacity (Hirunpraditkoon *et al*, 2011). Previous studies such as Ademiluyi *et al*, (2009) and Ijaola *et al*, (2013) remarked that AC is a good adsorbent with an exceptional ability to capture water dissolved contaminants, taste, odour, colour, and toxic pollutants. Its well-developed porous structure and tremendous surface area make it exceptional (Awoyale *et al*, 2013). Despite all these, the cost of the process is relatively expensive while using commercially available activated carbon. This challenge prompts more research on the preparation of AC from cheap or zero-cost starting materials such as agricultural products or by-products such as olive stones, almond shells, apricot and peach stones, maize cob, linseed straw, sawdust, rice hulls, cashew nut hull, cashew nut sheath, coconut shells, and husks (Nam *et al*, 2018). Agricultural products such as eucalyptus bark, linseed cake, tea waste ash, pecan shell, sugarcane bagasse, and bamboo are useful by-products, considered an effective alternative to the existing commercial AC. The adsorption capacity of a pyrolyzed bamboo can further be enhanced by an activation process which could either be a physical or chemical process. In physical activation, the carbonized bamboo is activated in the presence of air and activating gases such as carbon dioxide and (steam) (Moreno-Castilla *et al*, 2011). For chemical activation, several types of chemicals that may include $ZnCl_2$, H_3PO_4, HNO_3, KOH, etc. are used as the activating agent (Moreno-Castilla *et al*, 2011). Both carbonization and activation processes occur simultaneously at a lower temperature and a shorter time than in physical activation. Chemical activation gives activated carbon a higher specific surface area and much better-developed porosity than physical activation (Hirunpraditkoon *et al*, 2011). The structural characterization and surface morphology of AC can be determined through different methods of analysis such as Fourier Transform Infrared Spectroscopy (FTIR), Scanning Electron Microscopy (SEM), X-ray fluorescence spectrometry (XRF), X-Ray Diffraction (XRD) and these have been well documented by Dutrow and Clark (2019) and Topare and Joshi (2016).

The Physico-chemical properties of bamboo, along with mechanical properties are perhaps the reason why bamboo has gained more global attention as major material for the production of AC rather than wood. The objective of this study, was to produce charcoal from bamboo (*Bambusa vulgaris*), activate the charcoal using trioxonitrate (V) acid (HNO_3) and potassium hydroxide (KOH) and characterize the activated carbon through Fourier Transform Infrared Spectroscopy (FTIR) and Scanning Electron Microscopy (SEM) methods.

II. METHODOLOGY

A. Production of Activated Carbon

Bamboo stems were harvested from the Federal College of Agriculture Akure, Akure, Nigeria (Latitude 7.30 °N and Longitude 5.14 °E). The city has a tropical humid climate with two distinct seasons, a relatively dry season from November - March and a rainy season from April - October. Average annual rainfall ranges from 1405 to 2400 mm while atmospheric temperature ranges from 28 °C to 31°C with a mean annual relative humidity of about 80% in April when the rainy season begins. Akure is about 351 m above mean sea level with an area of about 2,303 km^2, situated within the western upland area (Akinbile *et al*, 2016).

The freshly harvested stems, resized into smaller pieces (averaging 4 cm x 4 cm) before the commencement of carbonization. The carbonization process was carried out at a temperature ranging from 260 ℃ to 300 ℃ in a muffle furnace resulting in the formation of non-volatile carbon using the procedure outlined in Zhou (1998), and the product was allowed to cool at room temperature. The carbonized bamboo was then divided into three to create a 3-variable experiment. One sample was left untreated as the control experiment (inactivated carbon) while the remaining two samples were activated with 0.4 M of KOH and 0.4 M of HNO_3 respectively following standard procedure. All the samples were characterized using Fourier Transfer Infrared Spectroscopy (FTIR) and Scanning Electronic Microscope (SEM) to identify the chemical functionality and surface physical morphology.

B. Fourier Transfer Infrared Spectroscopy (FTIR)

The FTIR spectroscopy was initially used for qualitative and quantitative analysis of organic compounds by providing specific information on molecular structure, chemical bonding, and molecular environment (Gerwert and Kotting, 2010) but it is now used on solids, liquids, or gases to identify their functional groups by obtaining an infrared spectrum of absorption or emission from such material. In identifying functional groups in the three adsorbents, the activated carbonated charcoal, HNO_3 AC, and KOH AC, were measured in a range of 4000 to 400 cm^{-1} using potassium chloride disks containing 1% finely granule samples on a Nicolet 550 FTIR spectrometer (Thermostatic Nicolet. Waltham, Ma, USA). The FTIR investigated the vibration of molecules and polar bonds between the different atoms, types of bonds, and functional groups.

C. Scanning Electronic Microscopy (SEM)

The surface morphology of the adsorbents was identified using the Phenon Prox Scanning Electronic Microscopy (SEM) machine. The samples were sprinkled on the sample stub laid with double adhesive and moved to a sputter coater (quorum-Q150R plus E) with 5nm of gold, placed on a charge reduction sample holder, and introduced into the column of the SEM machine. This process was repeated for the different adsorbents and during the process of identification, a high-energy electron beam was allowed to scan across the surface of all the adsorbents. While the scanning process was on, interactions between the samples and electron beam resulted in different types of electron signals being emitted on the sample's surface. These electronic signals were collected, processed, and translated as pixels on a monitor to form an image of the samples' surface.

D. Analysis of Data

Results obtained were subjected to statistical analysis using the SPSS version 16 for descriptive analysis, analysis of variance (ANOVA) and the post hoc test with Least Significant Difference (LSD), and Duncan Multiple Range Test at a 95% level of significance.

III. RESULTS AND DISCUSSION

The characterization of three adsorbents (inactivated carbonized charcoal, HNO_3, AC and KOH AC) was characterized using Fourier Transform Infrared Spectroscopy (FTIR) and Scanning Electronic Microscope (SEM) techniques.

A. Adsorbents' characterization using Fourier Transform Infrared Spectroscopy (FTIR)

The spectra profile and relative intensity of infrared (IR) bands for both the inactivated carbon and the activated carbons are shown in Figures 1 through 3. The spectra interpretation of the functional groups found to be present in the samples were presented in Table 1.

The FTIR spectra peaks of bamboo charcoal bits which was carbonated at 300^0C (Figure 1) were 3388.2 cm^{-1}, 3364.8 cm^{-1}, 2122.7 cm^{-1}, 1619.5 cm^{-1}, 1507.7 cm^{-1}, 1541.3 cm^{-1}, 1436.9 cm^{-1}, 1364.2 cm^{-1} and 1084.7 cm^{-1}. These bands were classified into seven absorption bands 3570-3320 cm^{-1} (O-H stretch of Hydroxyl group), 2140-2100 cm^{-1} (Terminal alkyl monosubstituted), 1650-1600 cm^{-1} (Conjugated ketone stretch), 1555-1485 cm^{-1} (Aromatic Nitro compounds), 1470-1430 cm^{-1} (Methyl C-H bend), 1380-1350 cm^{-1} (Aliphatic Nitro compound Stretch) and 1140-1070 cm^{-1} (Alkyl substituted ether C-O stretch) as explained by Coates (2000) and further confirmed by Wang *et al*, (2020b). Broadband at 3570-3320 cm^{-1} with two peaks 3388.2 cm^{-1} and 3364.8 cm^{-1} due to the absorption of water molecules as a result of an O-H stretching mode of hydroxyl groups (Zhang *et al*, 2019). In the 2140-2100 cm^{-1} frequency group, terminal alkyl mono-substituted C≡C was observed on the charcoal with a peak of 2122.7 cm^{-1}. C=O conjugated ketone stretch was observed at the band 1650-1600 cm^{-1} with a peak of 1619.5 cm^{-1}.

Table 1: Spectra interpretation of the functional groups present in the adsorbents produced with reference to standard adsorption bands

S/N	Standard Adsorption bands (cm-1) and corresponding functional group Adapted from Coates. (2000)		Observed Adsorption bands in this study			Interpretations based on Coates. (2000)
	Standard adsorption bands (cm-1)	Functional groups	Adsorption bands in carbonated charcoal (cm-1)	Adsorption bands in HNO3 AC (cm-1)	Adsorption bands in KOH AC (cm-1)	Interpretation
1.	3570-3320 (Broad)	O-H	3388.2 3364.8		3328.5	Hydroxyl group, H bounded O-H stretch
2.	3360-3310	N-H		3319.2		Aliphatic secondary amine N-H stretch
3.	2240-2220	C≡N		2228.9		Aromatic Nitrile
4.	2140-2100	C≡C	2122.7	2100.4	2107.8	Terminal alkyne mono substituted
5.	2150-1990	N=C=S			2018.4	Iso-thiocyanate stretch
6.	1725-1700	C=O		1718.3	1718.3	Carboxylic acid C=O stretch (dimer)
7.	2000-1660	C-H		1919.6 1941.9	1984.8 1869.3	Aromatic C-H bend (overtone)
8.	1710-1685	C=O		1697.8		Conjugated acid stretch (dimer)
9.	1690-1675/ 1650-1600	C=C	1619.5	1684.8		Quinone or conjugated ketone stretch
10.	1680-1630			1636.3	1654.9	Amide group
11.	1630-1575	N=N		1576.7	1578.5	Open- chain azo (-N=N-)
12.	1555-1485/ 1355-1320	N=O	1507.7 1541.3	1522.6 1340	1507.7 1522.6 1541.3	Aromatic nitro compounds
13.	1470-1430/ 1380-1370	C-H	1436.9	1457.4 1375.4	1436.9 1375.4	Methyl C-H asym./sym. Bend
14.	1420-1410	C-H			1420.1	Vinyl C-H in plane bend
15.	1485-1445	C-H		1457.4	1459.3 1474.2	Methylene C-H bend
16.	1380-1350	N-O	1364.2	1094.0		Aliphatic nitro compound stretch
17.	1140-1070	C-O-C	1084.7		1105.2	Alkyl-substituted ether, C-O stretch
18.	1225-950	C-H		1209.5	1213.2	Aromatic C-H out-of-plane bend
19.	895-885	C=H		874.1		vinylidene C=H out-of-plane bend
20	890-820	C-O-O		855		Peroxide C-O-O stretch
21.	810-750	C=H		790.2 810.7		Aromatic C-H out-of-plane bend
22.	720-590	O-H		661.6 682.1	661.6	Alcohol, OH out-of-plane bend
23.	800-700	C-Cl		702.6 719.4 734.3	745.5	Aliphatic chloro compounds C-C stretch

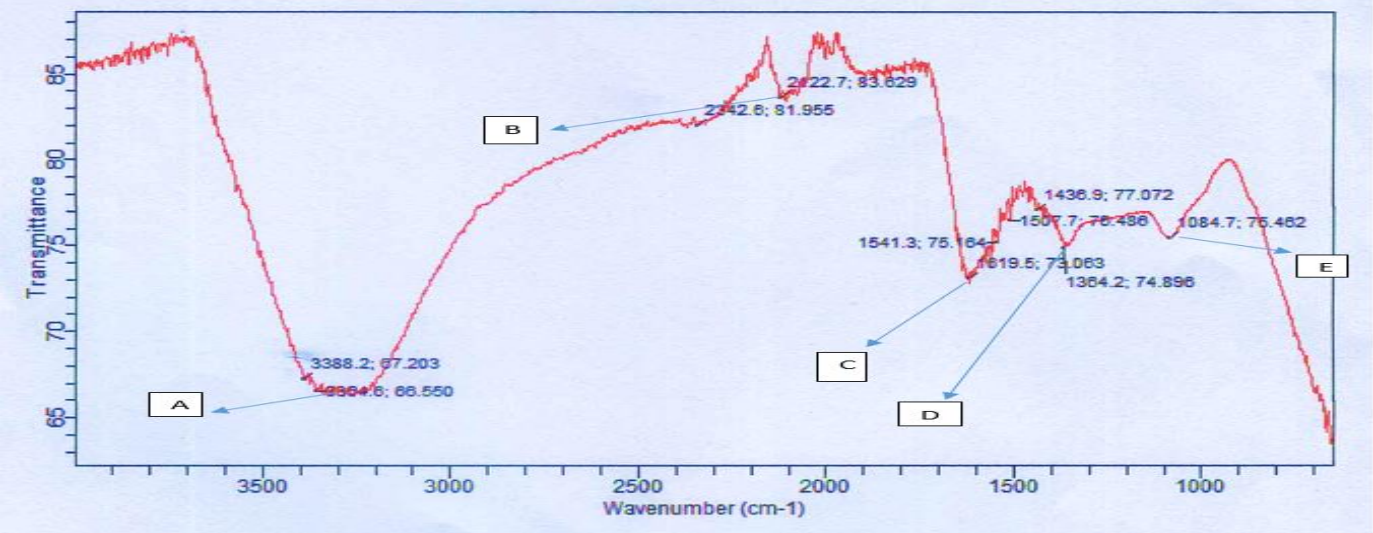

Figure 1: Results of FTIR imaging for carbonated charcoal showing the spectral peaks A – E

The band at 1555- 1485 cm^{-1} with two peaks 1507.7 cm^{-1} and 1541.3 cm^{-1} were assigned to aromatic nitro compounds. Peak of 1436.9 cm^{-1}, 1364.2 cm^{-1} and 1084.7 cm^{-1} c within the bands 1470-1430 cm^{-1}, 1380-1350 cm^{-1} and 1140-1070 cm^{-1} respectively. These bands were assigned with Methyl C-H bend, Aliphatic Nitro compound stretch, and Alkyl substituted ether C-O stretch, functional groups, respectively and further confirmed by Ma *et al*, (2019).

Figure 2 shows the spectra peaks of HNO_3 activated carbon spread across 18 absorption bands. A peak of 3319.2 cm^{-1} was observed within a broad band of 3360-3310 cm^{-1} that was assigned with aliphatic secondary amine N-H stretch. Small spectra bands like 2240-2220 cm^{-1} (Aromatic Nitrile) with 2228.9 cm^{-1} peak, 2140-2100 cm^{-1} (terminal mono substituted alkyne) with peak of 2100.4 cm^{-1}, and 1725-1700 cm^{-1} (Carboxylic acid C=O stretch (dimer)) with 1718.3 cm^{-1} were also observed. At band 2000-1660 cm^{-1} (Aromatic C-H bend overtone), two peaks of 1919.6 cm^{-1} and 1941.9 cm^{-1} were observed.

Various narrow bands like 1725-1700 cm^{-1} (Carboxylic acid C=O stretch dimer) with peak 1718.3 cm^{-1}, band 1710-1685 cm^{-1} (Conjugated acid stretch dimer) with peak 1697.8 cm^{-1}, 1690-1675/1650-1600 (Conjugated ketone stretch) with peak 1684.8 cm^{-1}, 1680-1630 cm^{-1} (Amide group) with peak 1636.3 cm^{-1}, 1630-1575 cm^{-1} (Open-chain azo -N=N) with peak 1576.7cm^{-1}, 1470-1430 cm^{-1} /1380-1370 cm^{-1} (Methyl C-H asym./sym. Bend) with peaks 1457.4 cm^{-1} and 1375.4 cm^{-1}, 1225-950 cm^{-1} (Aromatic C-H out-of-plane bend) with peak 1094.0 cm^{-1} and 1209.5 cm^{-1}, spectra band 895-885 cm^{-1} (vinylidene C=H out-of-plane bend) with peak 874.1 cm^{-1}, 890-820 cm^{-1} (Peroxide C-O-O stretch) with peak 855 cm^{-1}, 810-750 cm^{-1} (Aromatic C-H out-of-plane bend) with peaks 790.2 cm^{-1} and 810.7 cm^{-1}, 720-590 cm^{-1} (Alcohol, OH out-of-plane bend) with peaks 661.6 cm^{-1} and 682.1 cm^{-1} 800-700 cm^{-1} (Aliphatic chloro compounds C-C stretch) with three absorption peaks of 702.6 cm^{-1}, 719.4 cm^{-1} and 734.3 cm^{-1} were

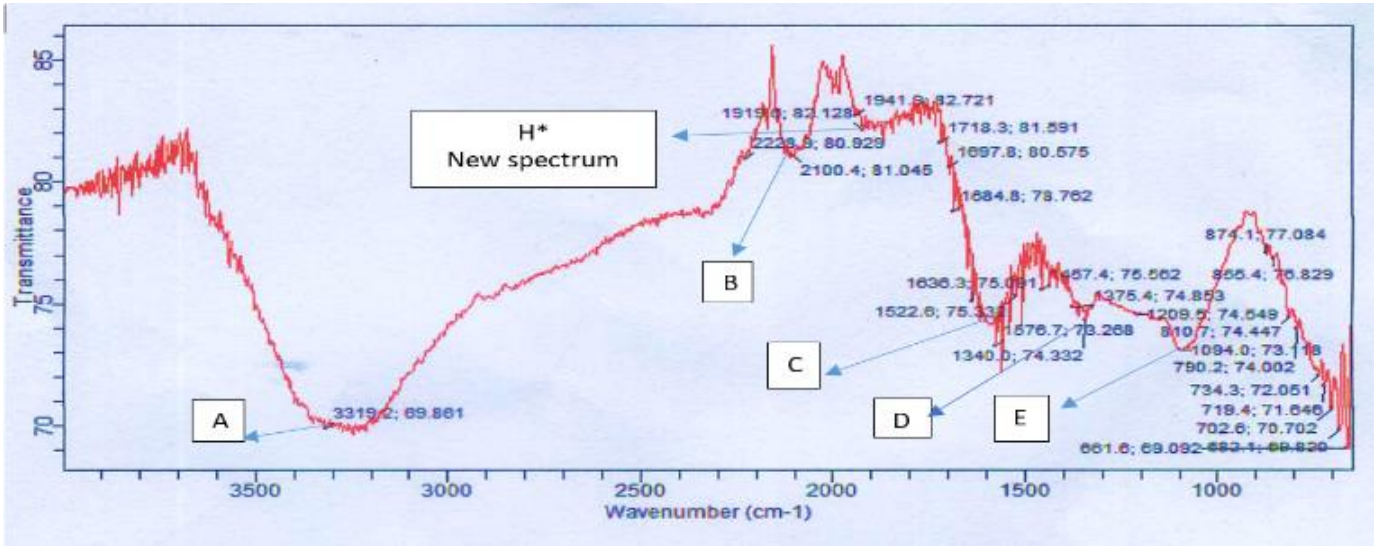

Figure 2: Results of FTIR imaging for HNO_3 Activated Carbon showing the spectral peaks A – E

also observed. Medium spectra band 1555-1485 cm^{-1}/ 1355-1320 cm^{-1} with two peaks which were 1522.6 cm^{-1} and 1340 cm^{-1} were equally observed which aligned with the findings of Chouikhi *et al,* (2021) who reported that identical spectra band with similar peaks were observed in their studies.

Figure 3 shows spectra peaks of KOH activated carbon with the spectra bands grouped into 15 different bands. A broadband 3570-3320 cm^{-1} (Hydroxyl group, H bounded O-H stretch) with 3328.5 cm^{-1} was observed. The following bands such as 2140-2100 cm^{-1} (Terminal alkyne monosubstituted) with a peak of 2107.8 cm^{-1}, 2150-1990 cm^{-1} (Iso-thiocyanate stretch) with peak 2018.4 cm^{-1}, 1725-1700 cm^{-1} (Carboxylic acid C=O stretch (dimer)) with a peak of 1718.3 cm^{-1}, 2000-1660 cm^{-1} (Aromatic C-H bend (overtone)) with peaks 1984.8 cm^{-1} and 1869.3 cm^{-1}, 1680-1630 cm^{-1} (Amide group) with 1654.9 cm^{-1}, 1630-1575 cm^{-1} (Open- chain azo (-N=N-)) with peak 1578.5 cm^{-1}, 1555-1485 cm^{-1}/ 1355-1320 cm^{-1} (Aromatic nitro compounds) with peaks. 1507.7 cm^{-1}, 1522.6 cm^{-1} and 1541.3 cm^{-1}, 1470-1430 cm^{-1}/1380-1370 cm^{-1} (Methyl C-H asym./sym. Bend) with peaks of 1436.9 cm^{-1} and 1375.4 cm^{-1}, 1420-1410 cm^{-1} (Vinyl C-H in-plane bend) with peak 1420.1 cm^{-1}, 1485-1445 cm^{-1} (Methylene C-H bend) with peaks 1459.3 cm^{-1} and 1474.2 cm^{-1}, 1140-1070 cm^{-1} (Alkyl-substituted ether, C-O stretch) with a peak of 1105.2 cm^{-1}, 1225-950 cm^{-1} (Aromatic C-H out-of-plane bend) with a peak of 1213.2 cm^{-1}, 800-700 cm^{-1} (Aliphatic chloro compounds C-C stretch) with a peak of 745.5 cm^{-1} and spectra band 720-590 cm^{-1} (Alcohol, OH out-of-plane bend) with a peak of 661.6 cm^{-1}. Moreover, the shifts and formation of new spectral on the activated carbons concerning the five major absorption bands (labeled A-E) on the charcoal (inactivated carbon) were observed as follows. The spectra in the broad region of 3388.2 cm^{-1} and 3364.6 cm^{-1} on inactivated charcoal (A of Figure 1) are related to the hydroxyl groups (–OH) that were shifted in KOH AC with 3328.5 cm^{-1} IR band (A of Figure 3).

The HNO_3 AC also shifted to 3319.2 cm^{-1} (A of Figure 2) but with a new assigned functional group of aliphatic secondary amine N-H stretch. Wang *et al,* (2020a) in their findings documented that broad absorption bands in the region (3650 cm^{-1} – 3250 $cm^{-1)}$ may be dominated by hydroxyl or amino groups but the presence of a nitrogenous base supports the amino classification. IR spectra 2122.7 cm^{-1}, 2100.4cm^{-1}, and 2107.8 cm^{-1} (B of Figures 1 through 3) with similar C≡C terminal alkyne mono substituted functional group was observed in the three adsorbents respectively. A new peak was formed at the 1984.8 cm^{-1} regions on KOH-activated carbon and was not prevalent on inactivated charcoal and HNO_3 AC (K* of Figure 3).

The peak shows the presence of an aromatic C-H bend (overtone). However, new peaks with a similar functional group were also noticed at 1919.6 cm^{-1} (H*of Figure 2) and 1869.8 cm^{-1} (K**of Figure 3) regions of HNO_3 AC and KOH AC respectively with no evidence of such group on carbonated charcoal. The next major IR band is at region 1619.5 cm^{-1} on carbonated charcoal (C of Figure 1) with assigned group Quinone or conjugated ketone of carbonyl group which was shifted to region 1522.6 cm^{-1} on HNO_3 AC (C of Figure 2) and 1578.5 cm^{-1} on KOH AC (C of Figure 3). The modification of the surface of these ACs gave assigned groups of the aromatic nitro group and Open chain azo group (-N=N) respectively. The IR band 1364.2 cm^{-1} on carbonated charcoal (D of Figure 1) of the aliphatic nitro compound stretch functional group was observed to have shifted on HNO_3 and KOH AC with peaks 1340.0 cm^{-1} (D of Figure 2) and 1375.4 cm^{-1} (D on Figure 3) and assigned functional group of an aromatic nitro compound. A new broadband 1213.2 cm^{-1} (K*** in Figure 3) assigned to the functional group of aromatic C-H out of plane bend was formed on KOH AC without such a new formation on carbonated charcoal and HNO_3 AC. The last major band on carbonated charcoal at region 1084.7 cm^{-1} with alkyl-

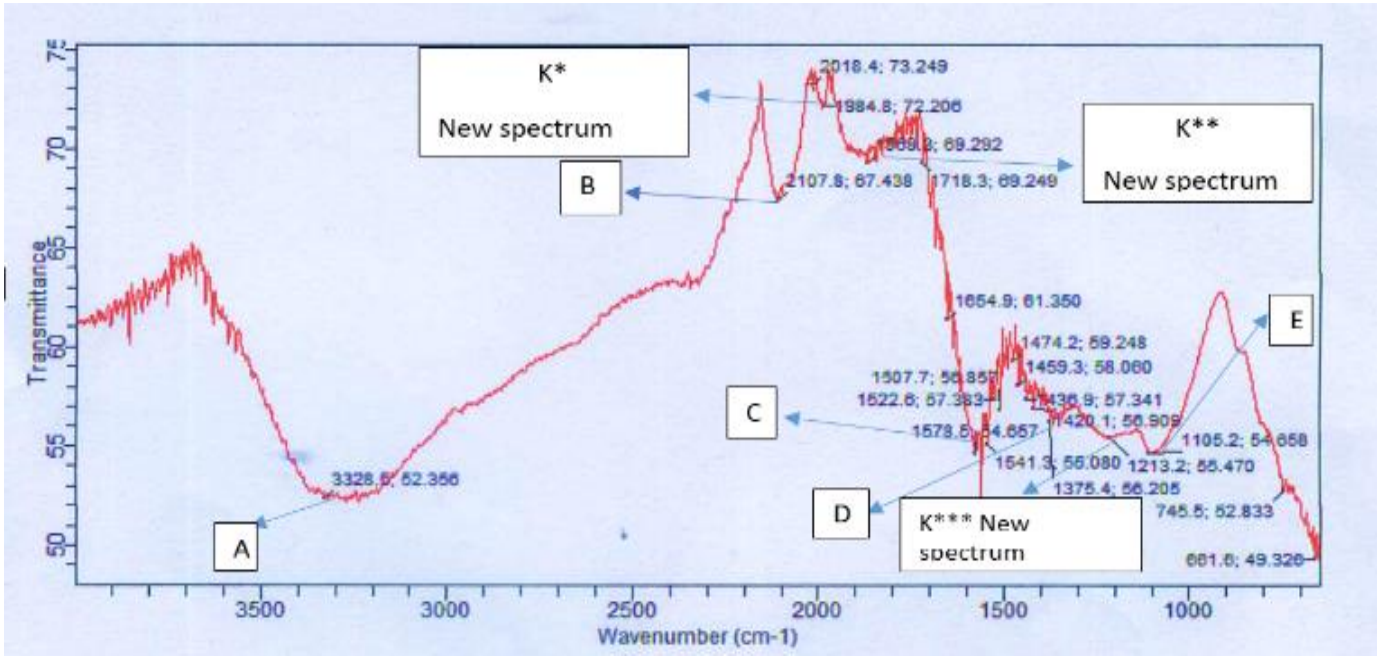

Figure 3: Results of FTIR imaging for KOH Activated Carbon showing the spectral peaks A – E, as well as K*, K and K*****

substituted ether functional group was shifted to region 1094.0 cm^{-1} on HNO_3 AC and 1105.2 cm^{-1} on KOH AC with a similar functional group.

From all the analyses and discussions of the FTIR results, KOH AC (Figure 3) was found to have more functional groups than both carbonated charcoal and HNO_3 AC and this could enhance its adsorption capacity. Khandaker *et al*, (2017) remarked that the adsorption of cations in the chemisorption process is generally enhanced by the existence of a higher amount of acidic functional groups on the adsorbent. However, the adsorbents were further subjected to a Scanning Electronic Microscope (SEM) analysis for investigating their adsorption capacities.

B. Adsorbents' characterization using Scanning Electronic Microscope (SEM)

The results of SEM imaging for the adsorbents at 300x, 500x, 1000x, and 1500x magnifications are shown in Figures 4 – 6 for carbonated charcoal (Figure 4a-d), HNO_3's AC (Figure 5a-d) and KOH's AC (Figure 6a-d).

In Figures 4a and 4b, the image shows distinct pore spaces observed in inactivated charcoal. Although the pore spaces were distinct, there was a poor visibility into the pore structure and inference on adsorption capacity and pore cavity size. However, for the 1000x (4c) and 1500x (4d) magnifications, there are finer details on the pore sizes, as well as evidence of the development of good pore structure and network. The pore sizes rank quite small though with quite a few pore walls collapsing, compared to the activated charcoal.

For the HNO_3 AC, the pore network and structure were better developed and were visible in the 300x and 500x magnification of Figures 5a and 5b respectively. Also observed are a few instances of pore walls collapsing in the image. A magnified view (Figure 5c and 5d) however confirms large pore spacing and size, and a well-distributed network and microstructure attributable to the effects of the activation process they underwent. Joshi *et al*, (2013) remarked that activating agents generally influences topographical characteristics of carbon surface especially the activated agents' surface area and porosity.

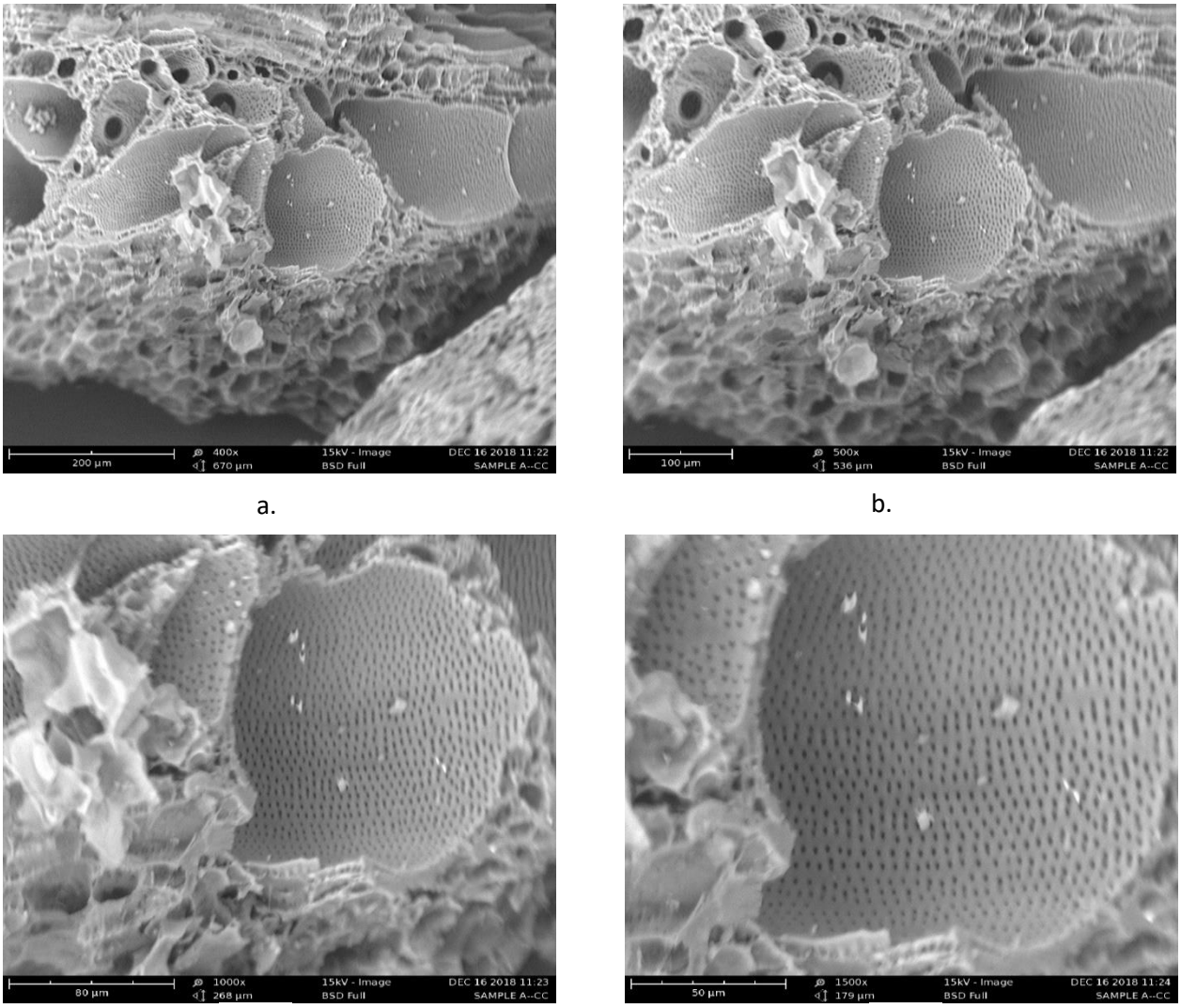

Figure 4a-d: Results of SEM imaging for Carbonated Charcoal at a. 300x, b. 500x, c. 1000x and d. 1500x magnification

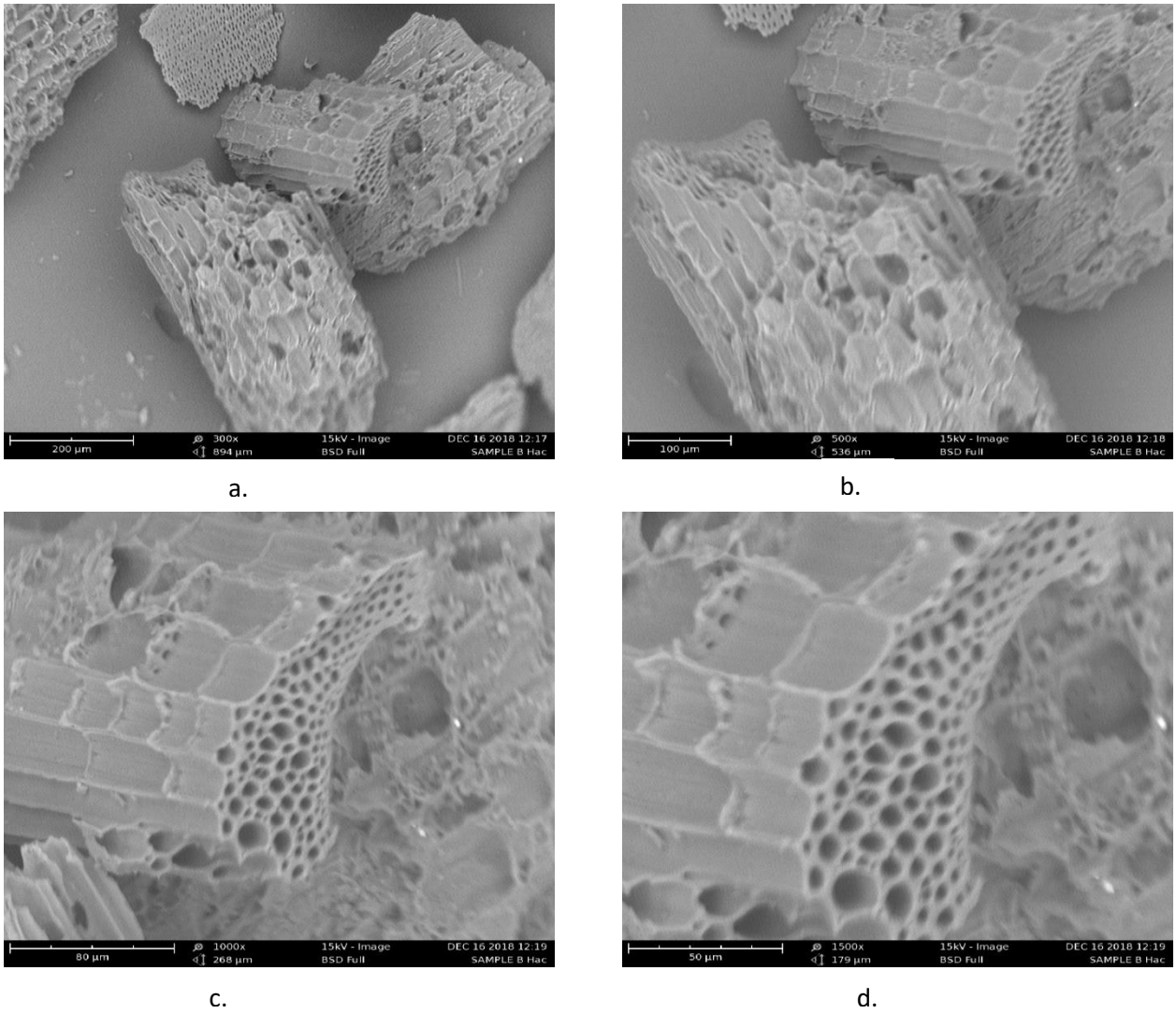

Figure 5a-d: Results of SEM imaging for HNO3 Activated Carbon at a. 300x, b. 500x, c. 1000x and d. 1500x magnification

Essentially, the presence of cavities increase the adsorption capacity, total available surface area and pore volume. This agrees with the findings of Nam *et al*, (2018) and Ilomuanya, (2017) that adsorptive characteristics of adsorbents vary with the physical characteristics such as internal total available surface area and micro/meso/macro-pore volume of the activated charcoal.

The surface of KOH-AC was observed to have well-developed pores (Figure 6a-d), with very minimal pore wall collapse. The higher magnification results in the latter images (6c, 6d) which showed well-developed longitudinal cavities, inferring high adsorption capacity, total internal volume and porosity. These well-developed pores are good potential for the adsorption of contaminants from wastewater. Joshi *et al*, (2013) suggested that with well-developed pores and cavities on the adsorbent, there is a better possibility for adsorption into the surface of the pores. Similarly, Mohan *et al*, (2007) remarked that AC prepared by KOH activation is highly microporous when compared to that produced through other activating agents like $ZnCl_2$ or H_3PO_4. Hirunpraditkoon *et al*, (2011) also noted that the use of KOH as an activating agent enabled activated carbon with greater specific surface area and pore volume relative to other activating agents.

Broadly, the low magnification imaging results and characterization of the adsorbents revealed the presence of pores on each adsorbent of various sizes. At 1500x magnification, the image clearly showed widespread pores in each of the samples showing the potential for all three adsorbents to absorb contaminants from wastewater albeit with differing capabilities. The HNO_3 and KOH AC had coarse rough surfaces, bigger pores, and cavities than inactivated charcoal. The KOH AC however, showed the most desired characteristics, and therefore was ranked as the best-activated carbon to adsorb contaminants from the three treatments explored.

IV. CONCLUSION

Bamboo charcoal is not only a great alternative for wastewater treatment, Bamboo charcoal is environmentally friendly, very useful in desalination processes and can help in pH regulation (Li *et al*, 2019; Masykuri and Purwanto, 2019; Ren *et al*, 2020) amongst others. The activation process improves and imparts desirable properties for better adsorption

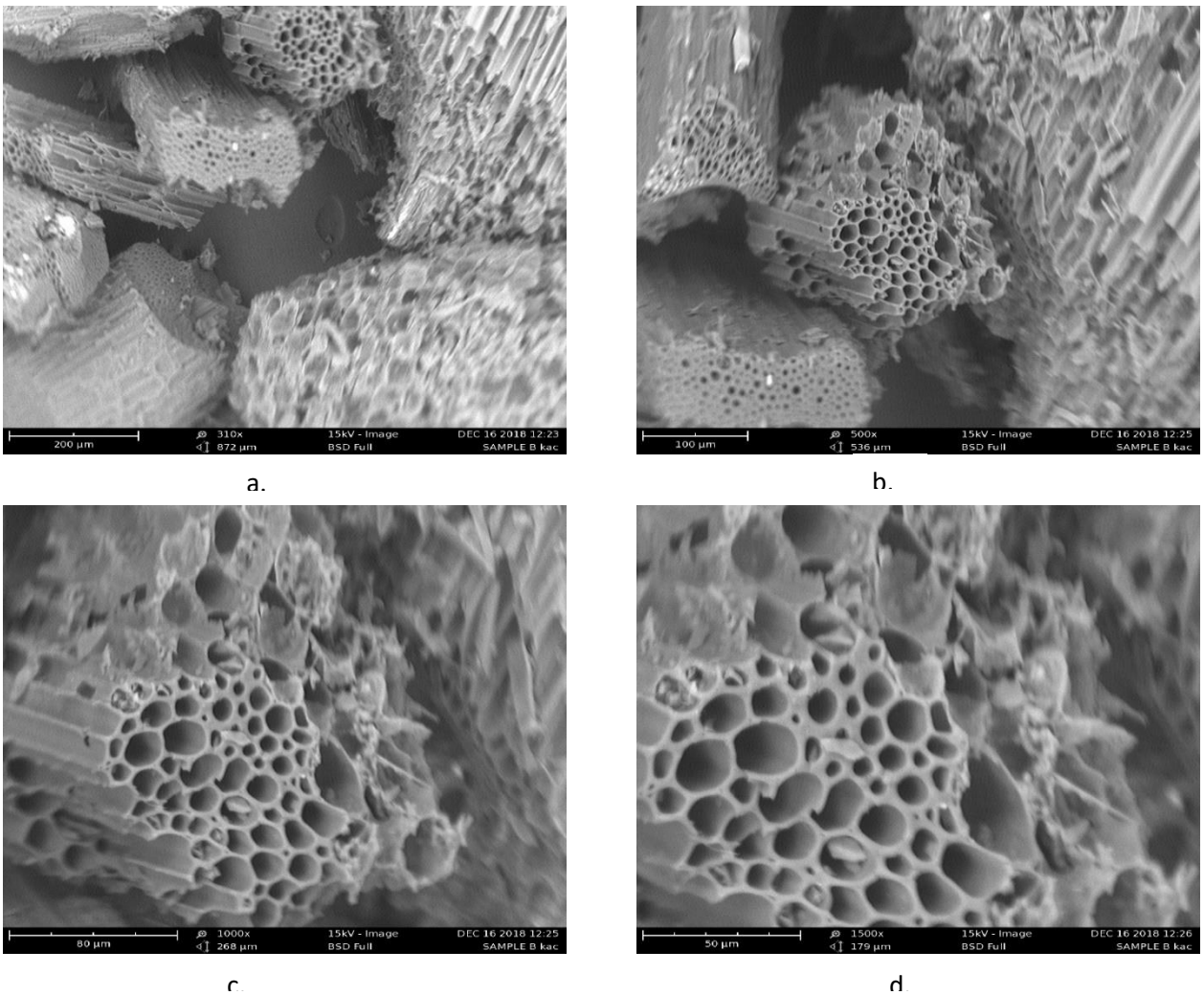

Figure 6a-d: Results of SEM imaging for KOH Activated Carbon at a. 300x, b. 500x, c. 1000x and d. 1500x magnification

and purification such as functional group presence and pore structure.

The differences in the number of spectra bands obtained for the three samples were 7, 18, and 15 bands for the inactivated bamboo charcoal, HNO_3 activated bamboo charcoal and KOH activated bamboo charcoal were clear distinction of the activation processes which underscored the advantage one had over the other. Although both AC samples had more functional groups, the SEM characterization allowed a deeper investigation into pore structure with details such as pore size, pore-volume, and pore network. As observed, the pore structure was generally better developed in the KOH AC relative to all other samples. Specifically, there was a better network in both KOH AC and HNO_3 AC. However, the better pore size such as diameter and pore volume of the KOH AC created good microporous (widespread and interconnected) structure giving it a clear advantage over the other two.

A synergy of both characterization indices shows that KOH AC has a performance advantage based on the examined properties. This translates to higher levels of adsorption and success in treating select wastewater, suggesting that higher removal efficiencies can be obtained at low cost using readily available bamboo. This study however clearly establishes that AC from bamboo has the desired characteristics for high adsorption levels and is an efficient low-cost technology for use in the waste-water treatment process.

DECLARATION OF INTERESTS

The authors declare that they have no known competing financial interests or personal relationships that could have appeared to influence the work reported in this paper.

ACKNOWLEDGEMENT(S)

The first author is grateful to the World Academy of Science (TWAS) which provided the funds for this study under the COMSTECH-TWAS Joint Research Grants Programme. Ref.: 15-276 RG/ENG/AF/AC_C – FR3240288935 and to the Federal University of Technology, Akure (FUTA) which provided other logistics to successfully carry out the study. The contributions of the anonymous reviewers are also gratefully appreciated.

AUTHOR CONTRIBUTIONS

C.O. Akinbile: conceptualization, methodology and supervision, review and editing, **E. M. Epebinu:** experimentation, instrumentation, software usage and original draft writing, **O. O. Olanrewaju:** co-supervision and review,

A. T. Abolude: review and editing, layout and methodology validation

REFERENCES

Ademiluyi, F. T.; S. A. Amadi, and N. J. Amakama (2009). Adsorption and Treatment of Organic Contaminants using Activated Carbon from Waste Nigerian Bamboo. Journal of Applied Science and Environmental Management, 13 (3): 39 – 47.

Akinbile C.O.; A.E. Erazua; B. E. Babalola and F. Ajibade. (2016). Environmental Implications of Animal Wastes Pollution on Agricultural Soil and Water Quality, Soil and Water Research, 11 (3): 172-180.

Awoyale, A.A.; A.C. Eloka-Eboka and A.O. Odubiyi, (2013). Production and Experimental efficiency of activated carbon from local waste bamboo for wastewater treatment. International Journal of Engineering and Applied Sciences. 3 (2): 08 – 17

Chouikhi, N.; J. A. Cecilia; E. Vilarrasa-García; L. Serrano-Cantador; S. Besghaier; M. Chlendi; M. Bagane and R. Castellón, E. (2021). Valorization of agricultural waste as a carbon material for selective separation and storage of CO_2, H_2 and N_2, Biomass and Bioenergy, 155, 106297 -106304 https://doi.org/10.1016/j.biombioe.2021.

Coates, J. (2000). Interpretation of Infrared Spectra, A practical approach. Encyclopedia of Analytical Chemistry. R.A. Meyers (Eds), 10881-10882.

Dutrow, B.L, and Clark, C.M. (2019). Geochemical Instrumentation and Analysis. *Assessed from https://serc.carleton.edu/research_education/geochemsheets/techniques/XRD.html on 4th February 2019.*

Gerwert, K, and Kotting, C. (2010). Fourier Transform Infrared Spectroscopy (FTIR). In els, (Ed.) 12-18.

Hirunpraditkoon S.; T. Nathaporn; R. R. Anotai and N. Kamchai (2011). Adsorption Capacities of Activated Carbons Prepared from Bamboo by KOH Activation. World Academy of Science, Engineering and Technology International Journal of Chemical, Molecular, Nuclear, Materials, and Metallurgical Engineering 5 (6): 477-481.

Ijaola, O. O.; K. Ogedengbe and A.Y. Sangodoyin (2013). The Efficacy of Activated Carbon Derived from Bamboo in the Adsorption of Water Contaminants. International Journal of Engineering Inventions e-ISSN: 2278-7461, p-ISBN: 2319-6491 2(4): 29-34.

Ilomuanya M. O.; B. Nashiru; N. D. Ifudu and C. I. Igwilo (2017). Effect of pore size and morphology of activated charcoal prepared from midribs *of Elaeis guineensis* on adsorption of poisons using metronidazole and *Escherichia coli* O157: H7 as a case study. *Journal of Microscopy and Ultrastructure* 5 (1): 32-38.

Isa, S.S.M.; M. M. Ramli; N.A.M.A. Hambali; S.R. Kasjoo; M.M. Isa; N.I.M. Nor; N. Khalid and N. Ahmad (2016). Adsorption properties and potential applications of bamboo charcoal: A review. DOI: 10.1051/matecconf/20167801097.

Isa, S.S.M.; M. M. Ramli; D.S.C. Halim; N.A.M. Anhar and N.A.M.A. Hambali (2017). Different carbonization processes of bamboo charcoal using *Gigantochloa albociliata.* AIP conference proceedings 1885, 020226; DOI: 10.106311.5002420

Jiang, S. (2004). Training Manual of Bamboo Charcoal for Producers and Consumers. Bamboo Engineering Research Center. Nanjing Forestry University.

Joshi S.; M. Adhikari; B. P. Pokharel and R.R. Pradhananga (2013). Effects of Activating Agents on the Activated Carbons Prepared from Lapsi Seed Stone. Research Journal of Chemical Sciences. 3 (5): 19-24.

Khandaker S.; T. Kuba; Y. Toyohara; S. Kamida and Y. Uchikawa (2017). Development of ion-exchange properties of bamboo charcoal modified with concentrated nitric acid. IOP Conf. Series: Earth and Environmental Science 82 (2017) 012002, 3rd International Conference on Water Resource and Environment (WRE 2017).**Li, Z.; C. Wang; T. Lei; H. Ma; J. Su; S. Ling and W. Wang (2019).** Arched bamboo charcoal as interfacial solar steam generation integrative device with enhanced water purification capacity. Advanced Sustainable Systems, 3 (4): 1800144 - 1800153.

Ma, Z.; Y. Zhang; Y. Shen; J. Wang; Y. Yang; W. Zhang and S. Wang (2019). Oxygen migration characteristics during bamboo torrefaction process based on the properties of torrefied solid, gaseous, and liquid products, Biomass and Bioenergy, 128, 105300 – 105312, https://doi.org/10.1016/j.biombioe.2019.105300.

Masykuri, M. and Purwanto, E. (2019). Batik Industry Wastewater Treatment Using Fito Remediation of Water Hyacinth with Adsorbent consist of Organic Waste Bagasse, Rice Husks and Bamboo Charcoal. in *IOP Conference Series:* Materials Science and Engineering, 1. 508 (1): 012). IOP Publishing.

Mohan D.; P. K. Singh and K. V. Singh (2007). Wastewater Treatment Using Low-Cost Activated Carbons Derived from Agricultural Byproducts – A case study, Journal of Hazardous Materials. DOI: 10.1016/j.jhazmat.2007.07.079

Moreno-Castilla, C.; F. Carrasco-Marín; M.V. López-Ramón and M.A. Alvarez-Merino (2011) Chemical and physical activation of olive mill wastewater to produce activated carbons, Journal of Hazardous materials, (39):1415-1420

Nam, H.; W. Choi; A. Divine; S.C. Genuino and A. Capareda (2018a). Development of rice straw activated carbon and its utilizations, *Journal of Environmental Chemical Engineering*, 6 (4): 5221-5229**Nam, H.; S. Wang and H.R. Jeong (2018b).** TMA and H_2S gas removals using metal loaded on rice husk activated carbon for indoor air purification. *Fuel*, *213*, 186-194.

Omiyale, O. (2013). Bamboo and Rattan: vehicle for poverty alleviation in Nigeria. XII world forestry congress, 2003. Quebec City, Canada. 1015-A1

Ren, Q.; Z. Zeng; Z. Jiang and H. Li (2020). Functionalization of renewable bamboo charcoal to improve indoor environment quality in a sustainable way. Journal of Cleaner Production, 246, 119028 -119035.

Topare, N. and Joshi, P. (2016). Characterization of Activated Carbon Prepared from Citrus Sinensis (Orange) Peels by X-Ray Fluorescence Spectroscopy (XRF). Journal of Emerging Trends in Chemical Engineering, 2 (3): 49-51

Wang, Y.; C. Peng; E. Padilla-Ortega; A. Robledo-Cabrera; A. López-Valdivieso, (2020a). Cr (VI) adsorption on activated carbon: Mechanisms, modeling and limitations in water treatment, *Journal of Environmental Chemical Engineering*, *8*, (4): 104031 -104039

Wang, S.; H. Nam; H. Nam (2020b). Preparation of activated carbon from peanut shell with KOH activation and its application for H_2S adsorption in confined space *Journal of Environmental Chemical Engineering*, 8 (2): 103683 -103692

WWAP (United Nations World Water Assessment Programme) (2017). The United Nations World Water Development Report 2017. *Wastewater: The Untapped Resource*. Paris, Published by United Nations Educational, Scientific and Cultural Organization (UNESCO): pp 16-26

Zhang, X.; X. Mao; L. Pi; T. Wu; Y. Hu (2019). Adsorptive and capacitive properties of the activated carbons derived from pig manure residues, *Journal of Environmental Chemical Engineering*, *7* (3): 103066 - 103074

Zhou, F. (1998). Bamboo forest cultivation. China Forestry Publishing House. Beijing, China. 105pp